Influence of Wall Flexibility on Seismic Earth Pressures in Vertically Homogeneous Soil

Scott J. Brandenberg, Ph.D., P.E., M.ASCE,[1] Jonathan P. Stewart, Ph.D., P.E., F.ASCE,[2] and George E. Mylonakis, Ph.D., M.ASCE[3]

[1]Department of Civil and Environmental Engineering, University of California, Los Angeles, 5731 Boelter Hall, Los Angeles, CA 90095; e-mail: sjbrandenberg@ucla.edu
[2]Department of Civil and Environmental Engineering, University of California, Los Angeles, 5731 Boelter Hall, Los Angeles, CA 90095; e-mail: jstewart@seas.ucla.edu
[3]Department of Civil Engineering, University Walk, Clifton BS8, Bristol, U.K.; Professor, Univ. of Patras, Greece; Adjunct Professor, Dept. of Civil and Environmental Engineering, 5731 Boelter Hall, Univ. of California, Los Angeles, CA 90095-1593. Email: g.mylonakis@bristol.ac.uk

ABSTRACT

Solutions are formulated for seismic earth pressures acting on vertical flexible walls with the top and bottom constrained by discrete elastic stiffness elements (top constraint representing a structural constraint, bottom constraint representing foundation stiffness). Solutions are formulated using the Winkler assumption and correspond to shear waves propagating vertically through homogeneous soil. Earth pressures decrease as wall flexibility increases. Rotational and translation constraints at the top and bottom of the wall also contribute to mobilization of seismic earth pressures. Current standard-of-practice procedures are based on limit analysis methods that do not consider the influence of frequency, wall flexibility, structural constraints, or soil-structure interaction (SSI) in general. The proposed approach is more robust because wave propagation effects are considered and seismic earth pressures result from the product of relative wall-soil displacements and stiffness at the wall-soil interface.

INTRODUCTION

Seismic earth pressures acting on free-standing retaining walls and shallowly embedded structures are commonly computed using a limit analysis in which a pseudo-static seismic coefficient (k_h) acts upon an active Coulomb-type wedge in frictional soil, which results in an incremental change in the lateral earth pressure coefficient, K_{AE}, over its static counterpart, K_A. This approach is based on research by Okabe (1924) and Mononobe and Matsuo (1929), and is commonly known as the "Mononobe-Okabe" (M-O) method. Seed and Whitman (1970) observed that the M-O solution was approximately linear in the range of k_h from 0 to 0.4, and

suggested a simplified linear form of the equation. Recent centrifuge experiments (Al Atik and Sitar 2010, Mikola et al. 2016) support a linear relationship between k_h and K_{AE}, with the Seed and Whitman method providing a good match for braced non-displacing basement walls, and lower pressures for free-standing retaining walls and cantilever basement walls. Furthermore, the seismic earth pressure distribution from the centrifuge tests was interpreted as being triangular in shape, which results in less bending moment demand than the typical assumption that the resultant acts at $0.6H$ from the base of the wall (e.g., Mononobe and Matsuo 1929), where H is wall height. An important finding from those centrifuge tests was that wall flexibility and base sliding significantly influenced mobilized seismic earth pressures. Limit analysis procedures do not consider these structural characteristics because relative wall-soil displacement is not considered in their formulation.

Elasto-dynamic solutions provide an alternative to limit analysis procedures. Typically, elasto-dynamic solutions are based on a vertically propagating shear wave acting on a vertical rigid wall. Furthermore, the retained soil is taken as an elastic soil layer resting on a rigid base, and the soil layer thickness is the same as the wall height (i.e., the "bathtub" configuration). Notable examples of this method are Wood (1973), Arias et al (1981), Veletsos and Younan (1994), Younan and Veletsos (2000), Ostadan (2005), Papazafeiropoulos and Psarropoulos (2010), Kloukinas et al. (2012) and Vrettos et al. (2016). These methods tend to produce seismic earth pressures that are higher than M-O pressures because: (1) the wall is usually assumed to be rigid, (2) the soil layer is excited at its first-mode frequency, producing significant depth-variations in ground motions, which in turn produce large relative wall-soil displacements.

Brandenberg et al. (2015) demonstrated that kinematic seismic earth pressures have a strong dependence on the wavelength-to-height ratio (λ/H) and high values of λ/H are associated with lower earth pressures. Most walls are not founded on a rigid base, and the ground motion mean period tends to be associated with high λ/H values that often produce low seismic earth pressures. Although elasto-dynamic solutions are typically formulated for rigid walls and uniform soils, there are exceptions. Younan and Veletsos (2000) studied flexible cantilever and braced walls in the "bathtub" configuration, and found that wall flexibility tends to decrease seismic earth pressures compared with rigid walls. In the limit case of a perfectly flexible wall, seismic earth pressures are naturally zero at all wavelength-to-height ratios λ/H. This physical constraint cannot be captured by limit analysis solutions. Furthermore, earth pressures mobilized against cantilever walls tend to become more triangular as the walls become more flexible. Vrettos et al. (2016) formulated essentially exact analytical solutions for the "bathtub" configuration, but with vertically inhomogeneous soil. Their solutions show that earth pressures tend to increase with depth, whereas elasto-dynamic solutions with uniform soil tend to predict that earth pressures are highest at the surface (a trend also confirmed by numerical analyses, Ostadan, 2005).

A clear research need is to establish solutions for flexible walls retaining vertically inhomogeneous soil, and to move away from the "bathtub" configuration towards more realistic geometries and boundary conditions. The purpose of this paper is to demonstrate the influence of wall flexural stiffness and top/base constraint on seismic earth pressures for cantilever and braced walls. Solutions are based on two assumptions: (1) soil reactions at different depths are uncorrelated (classical Winkler assumption), and (2) excitation is from vertically propagating shear waves. Both assumptions are not essential and can be relaxed in future research to accommodate continuity in the soil reaction at different depths through higher-order models, as well as inclined seismic waves. To facilitate closed-form solutions of the governing ordinary differential equation, the soil is treated as uniform.

PROBLEM STATEMENT

Fig. 1 shows the geometry of the considered wall-soil configuration. An underground structure consisting of rigid diaphragms and flexible walls is embedded in a uniform soil profile undergoing seismic excitation by vertically propagating shear waves. This schematic includes intermediate walls and a roof diaphragm. These elements may not exist for some structures, but are included in the figure and derivation presented herein. The structure is embedded with its top flush with the ground surface. Underground structures are often embedded with the top below the surface, but this scenario is not considered here. However, the proposed solution procedure could easily be adapted for application to underground structures, provided that appropriate stiffness intensity values are derived, and the free-field ground motion is appropriate for the depth range of the walls. The assumption of rigid roof and floor diaphragms is acknowledged as a limitation (particularly in bending) that may have significance in some cases. These elements are treated as rigid here to enable the base translational and rotational stiffness to be represented as discrete elements. Soil profiles often have shear stiffness increasing with depth, but these effects are not considered here to facilitate a reasonably simple closed-form solution.

The structure in Fig. 1 can be represented as a single vertical wall with translational and rotational constraints at the top and bottom, as illustrated in Fig. 2. The base translational and rotational stiffnesses arise from the rigid slab moving relative to the free-field soil, as indicated by Eqs. 1 and 2, where $V(H)$ is the base shear force, $M(H)$ is the base moment, u is the wall displacement, u_g is the free-field soil displacement, θ is wall rotation, K_{yb} is the base translational stiffness, and K_{xxb} is the base rotational stiffness. Note that the free-field rotation is zero for vertically propagating shear waves.

$$V(H) = K_{yb}\left[u(H) - u_{ff}(H)\right] \tag{1}$$

$$M(H) = K_{xxb} \cdot \theta(H) \tag{2}$$

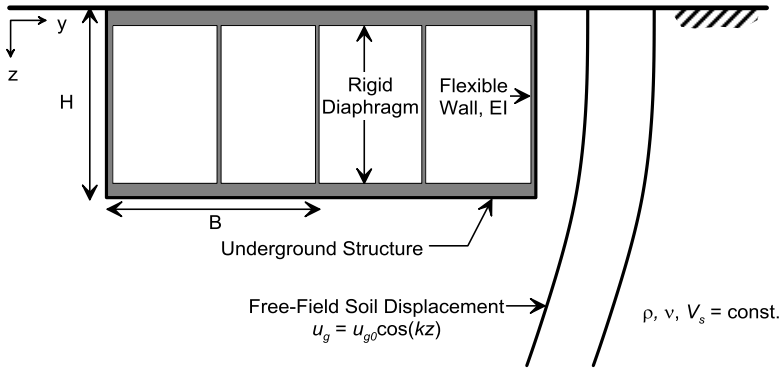

Figure 1. Schematic of underground structure consisting of vertical retaining walls, top and bottom diaphragms, and intermediate walls. The structure is subjected to a vertically-propagating shear wave in the free-field soil column.

The stiffness terms at the top of the wall represent structural resistance provided by the top diaphragm and the intermediate walls. By the principle of antisymmetry, the roof diaphragm does not provide a translational constraint under horizontal earthquake shaking unless it is connected to the floor diaphragm by intermediate structural elements. It can, however, provide a rotational constraint at the top of the wall. As illustrated in Fig. 2, forces at the top of the wall arise only from relative structural deformations between the base and top diaphragms, and rigid body deformation must be considered. The shear at the top of the wall, *V(0)*, and bending moment at the top of the wall, *M(0)*, are specified in Eqs. 3 and 4.

$$V(0) = K_{yt}\left[u(0) - u(H) + \theta(H)\cdot H\right] \tag{3}$$

$$M(0) = K_{xxt}\left[\theta(0) - \theta(H)\right] \tag{4}$$

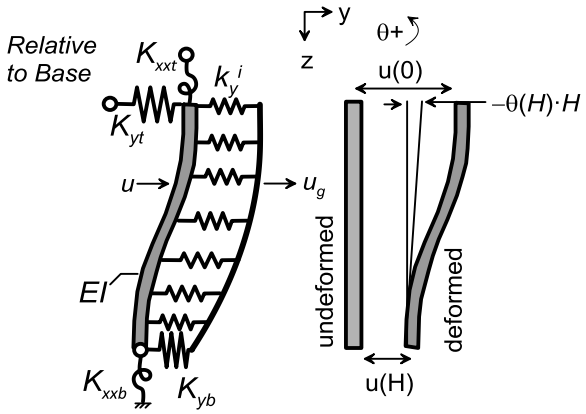

Figure 2. Winkler representation of wall with discrete stiffness at top and bottom, and distributed stiffness intensity along the length of the wall.

GOVERNING DIFFERENTIAL EQUATION

Assuming the flexible wall can be modeled as an Euler-Bernoulli beam with constant flexural stiffness, *EI*, and constant subgrade reaction stiffness intensity, k_y^i (horizontal stiffness per unit area), the differential equation governing kinematic soil-structure interaction between the wall and the vibrating soil column is given by Eq. 5.

$$EI\frac{\partial^4 u(z)}{\partial z^4} + k_y^i\left[u(z) - u_g(z)\right] = 0 \tag{5}$$

Note that inertial effects associated with the wall and structural elements are not considered; the influence of inertial soil-structure interaction would need to be addressed separately. Inertial effects associated with the soil are considered in the free-field site response and to the extent that k_y^i is frequency-dependent (e.g., Kloukinas et al. 2012).

The solution to this Eq. 5 is provided in Eq. 6, where $\beta = (k_y^i/4EI)^{0.25}$ is the Winkler constant, and $k = \omega/V_s$ is the wave number (Flores Berones & Whitman 1982, Rovithis et al 2012). Note that the moment of inertia, *I*, is computed per unit width of wall under the plane strain assumption [i.e. $t^3/12(1-\nu_w^2)$, where *t* is wall thickness and ν_w is the Poisson ratio for the wall material], and has units of L^3.

$$u(z) = C_1 e^{\beta z}\cos(\beta z) + C_2 e^{\beta z}\sin(\beta z) + C_3 e^{-\beta z}\cos(\beta z) + C_4 e^{-\beta z}\sin(\beta z) + \frac{k_y^i}{EI\cdot k^4 + k_y^i}u_{g0}\cos(kz) \tag{6}$$

Four boundary conditions at the two ends of the wall are specified to compute C_1, C_2, C_3, and C_4. For the problem at hand, the four boundary conditions arise from the stiffness terms at the base and top of the wall, and we solve for forces and displacements at the top and bottom of the wall rather than taking them as known boundary conditions. To impose the boundary conditions, derivatives of (6) with respect to *z* must first be computed, as provided in Eqs. 7-10. Note that in those equations $\theta = du/dz$, $M = EI\cdot d^2u/dz^2$, $V = EI\cdot d^3u/dz^3$, and $\Delta\sigma = EI\cdot d^4u/dz^4$. By making appropriate substitutions of (7) through (10) into (1) through (4), a system of equations (11) is obtained from which the values of C_1, C_2, C_3, and C_4 may be solved.

INFLUENCE OF WALL FLEXIBILITY AND TOP CONSTRAINT

Example solutions are presented in Figs. 3 through 5 for various values of βH for a case with the base fixed against rotation and translation, with various constraints at the top of the wall. Fig. 3 corresponds to a cantilever wall, Fig. 4 corresponds to a wall that is fixed against rotation at the connection with the top diaphragm, and Fig. 5 corresponds to a wall that is fixed against rotation

and translation at the connection with the top diaphragm. Solutions are plotted for $\lambda/H = 12$, which is generally consistent with experimental results by Al Atik and Sitar (2010). Note that first-mode resonance of the retained soil column corresponds to $\lambda/H = 4$, and would be associated with significantly higher earth pressures (Brandenberg et al. 2015).

Several general trends are evident from these figures. First, within each figure, wall displacements decrease while lateral earth pressures and bending moments increase as the wall becomes stiffer (i.e., as βH decreases). The increased pressure arises from larger relative displacements between the wall and the free-field soil. Second, comparing among the three figures, lateral earth pressures increase and wall displacements decrease as the constraint at the top of the wall increases. However, mobilized bending moments tend to decrease as constraints are added to the top of the wall because the wall exhibits double curvature when the top is constrained.

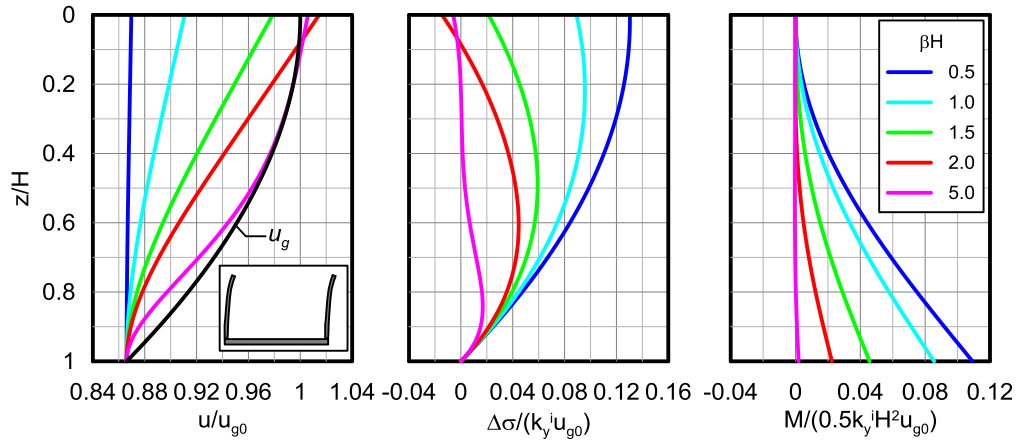

Figure 3. Solutions for displacement, seismic earth pressure increment, and bending moment for various values of βH and for $K_{yt} = K_{xxt} = 0$, and $K_{yb} = K_{xxb} = \infty$.

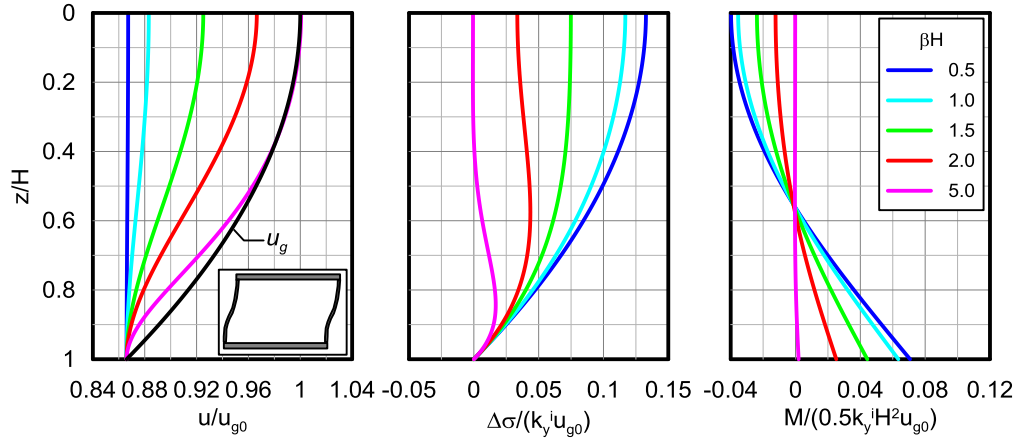

Figure 4. Solutions for displacement, seismic earth pressure increment, and bending moment for various values of βH and for $K_{yt} = 0$, and $K_{yb} = K_{xxb} = K_{xxt} = \infty$.

$$\frac{\partial u}{\partial z}=C_1\beta e^{\beta z}\left[\cos(\beta z)-\sin(\beta z)\right]+C_2\beta e^{\beta z}\left[\cos(\beta z)+\sin(\beta z)\right]-C_3\beta e^{-\beta z}\left[\cos(\beta z)+\sin(\beta z)\right]+C_4\beta e^{-\beta z}\left[\cos(\beta z)-\sin(\beta z)\right]-\frac{k_y^i\cdot k}{EI\cdot k^4+k_y^i}u_{g0}\sin(kz) \tag{7}$$

$$\frac{\partial^2 u}{\partial z^2}=-2C_1\beta^2 e^{\beta z}\sin(\beta z)+2C_2\beta^2 e^{\beta z}\cos(\beta z)+2C_3\beta e^{-\beta z}\sin(\beta z)+2C_4\beta^2 e^{-\beta z}\cos(\beta z)-\frac{k_y^i\cdot k^2}{EI\cdot k^4+k_y^i}u_{g0}\cos(kz) \tag{8}$$

$$\frac{\partial^3 u}{\partial z^3}=-2C_1\beta^3 e^{\beta z}\left[\cos(\beta z)+\sin(\beta z)\right]+2C_2\beta^3 e^{\beta z}\left[\cos(\beta z)-\sin(\beta z)\right]+2C_3\beta^3 e^{-\beta z}\left[\cos(\beta z)-\sin(\beta z)\right]+2C_4\beta^3 e^{-\beta z}\left[\cos(\beta z)+\sin(\beta z)\right]+\frac{k_y^i\cdot k^3}{EI\cdot k^4+k_y^i}u_{g0}\sin(kz) \tag{9}$$

$$\frac{\partial^4 u}{\partial z^4}=-4C_1\beta^4 e^{\beta z}\cos(\beta z)-4C_2\beta^4 e^{\beta z}\sin(\beta z)-4C_3\beta^4 e^{-\beta z}\cos(\beta z)-4C_4\beta^4 e^{-\beta z}\sin(\beta z)+\frac{k_y^i\cdot k^4}{EI\cdot k^4+k_y^i}u_{g0}\cos(kz) \tag{10}$$

$$\begin{bmatrix} K_{yb}e^{\beta H}C+2EI\beta^3e^{\beta H}(C+S) & K_{yb}e^{\beta H}S-2EI\beta^3e^{\beta H}(C-S) & K_{yb}e^{-\beta H}C-2EI\beta^3e^{-\beta H}(C-S) & K_{yb}e^{-\beta H}S-2EI\beta^3e^{-\beta H}(C+S) \\ K_{xxb}\beta e^{\beta H}(C-S)-2EI\beta^2e^{\beta H}S & K_{xxb}\beta e^{\beta H}(C+S)+2EI\beta^2e^{\beta H}C & -K_{xxb}\beta e^{-\beta H}(C+S)+2EI\beta^2e^{-\beta H}S & K_{xxb}\beta e^{-\beta H}(C-S)-2EI\beta^2e^{-\beta H}C \\ -K_{yt}\left(1-e^{\beta H}C\right)-2EI\beta^3-K_{yt}\beta He^{\beta H}(C-S) & K_{yt}e^{\beta H}S+2EI\beta^3-K_{yt}\beta He^{\beta H}(C+S) & -K_{yt}\left(1-e^{-\beta H}C\right)+2EI\beta^3-K_{yt}\beta He^{-\beta H}(C+S) & K_{yt}e^{-\beta H}S+2EI\beta^3-K_{yt}\beta He^{-\beta H}(C-S) \\ -K_{xxt}\beta+K_{xxt}\beta e^{\beta H}(C-S) & -K_{xxt}\beta+2EI\beta^2+K_{xxt}\beta e^{\beta H}(C+S) & K_{xxt}\beta-K_{xxt}\beta e^{-\beta H}(C+S) & -K_{xxt}\beta-2EI\beta^2+K_{xxt}\beta e^{-\beta H}(C-S) \end{bmatrix}\begin{Bmatrix} C_1 \\ C_2 \\ C_3 \\ C_4 \end{Bmatrix}= \tag{11}$$

$$\begin{Bmatrix} K_{yb}u_{g0}C-\dfrac{K_{yb}k_y^iu_{g0}C-EI\cdot k^3k_y^iu_{g0}S}{EI\cdot k^4+k_y^i} \\ \dfrac{K_{xxb}k\cdot k_y^iu_{g0}S+EI\cdot k^2k_y^iu_{g0}C}{EI\cdot k^4+k_y^i} \\ -\dfrac{K_{yt}k_y^iu_{g0}C-K_{yt}k_y^iu_{g0}+K_{yt}k\cdot H\cdot k_y^iu_{g0}S}{EI\cdot k^4+k_y^i} \\ \dfrac{K_{xxt}k\cdot k_y^iu_{g0}S+EI\cdot k^2k_y^iu_{g0}}{EI\cdot k^4+k_y^i} \end{Bmatrix}$$

$C=\cos(\beta H)$

$S=\sin(\beta H)$

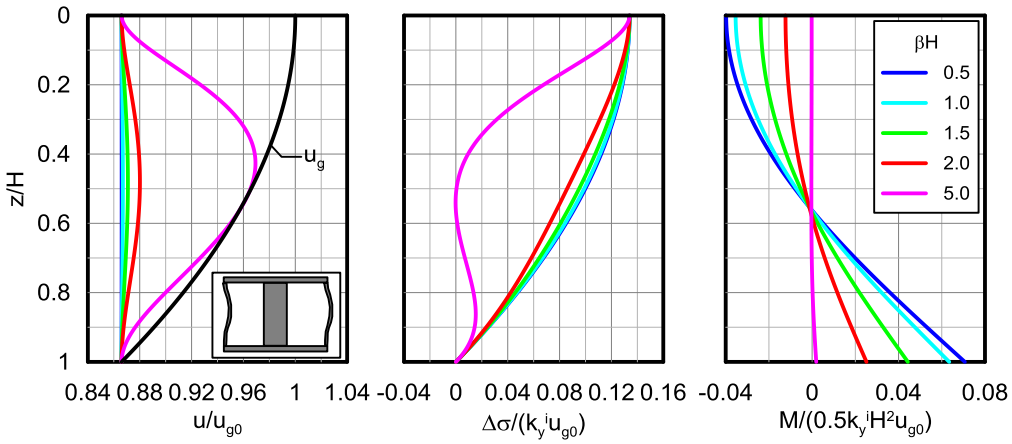

Figure 5. Solutions for displacement, seismic earth pressure increment, and bending moment for various values of βH and for $K_{xxt} = K_{yt} = K_{yb} = K_{xxb} = \infty$.

COMPARISON WITH YOUNAN AND VELETSOS (2000)

Younan and Veletsos (2000) developed an approximate analytical solution for the seismic earth pressure acting on flexible walls retaining uniform soil. Their solution corresponds to a "bathtub" configuration (i.e., $K_{yb} = K_{xxb} = \infty$), and they provided earth pressures for a static condition (i.e., a constant horizontal body force acting in the retained soil). They parameterized the wall stiffness using a dimensionless parameter d_w, which is related to βH as derived shown in Eq. 12, where ν_w and ν are the Poisson ratio for the wall and soil materials, respectively.

$$d_w = \frac{4(\beta H)^4 (1-\nu_w)}{\pi / \sqrt{(1-\nu)(2-\nu)}} \tag{12}$$

Figure 6(a) shows a comparison of the Younan and Veletsos solution with the proposed Winkler solution for the cantilever wall configuration. The solution is also compared with a finite element simulation performed using the program RS2 by Rocscience. The finite element solution was performed using a constant body force, and is provided as a point of reference for the two approximate analytical solutions. Details of the mesh configuration cannot be presented here due to length considerations. Earth pressures computed from the proposed Winkler solution are slightly larger than those from the Younan and Veletsos solution for stiff walls (d_w = 0 and 1) and slightly lower than those for flexible walls (d_w = 5 and 40). The finite element solution lies between the two approximate analytical solutions, but is closer to the Younan and Veletsos solution. In these analyses the spring values k_y^i derived by Kloukinas et al. (2012) for rigid walls were employed. Wall flexibility likely influences k_y^i, but this effect is beyond the scope of this paper.

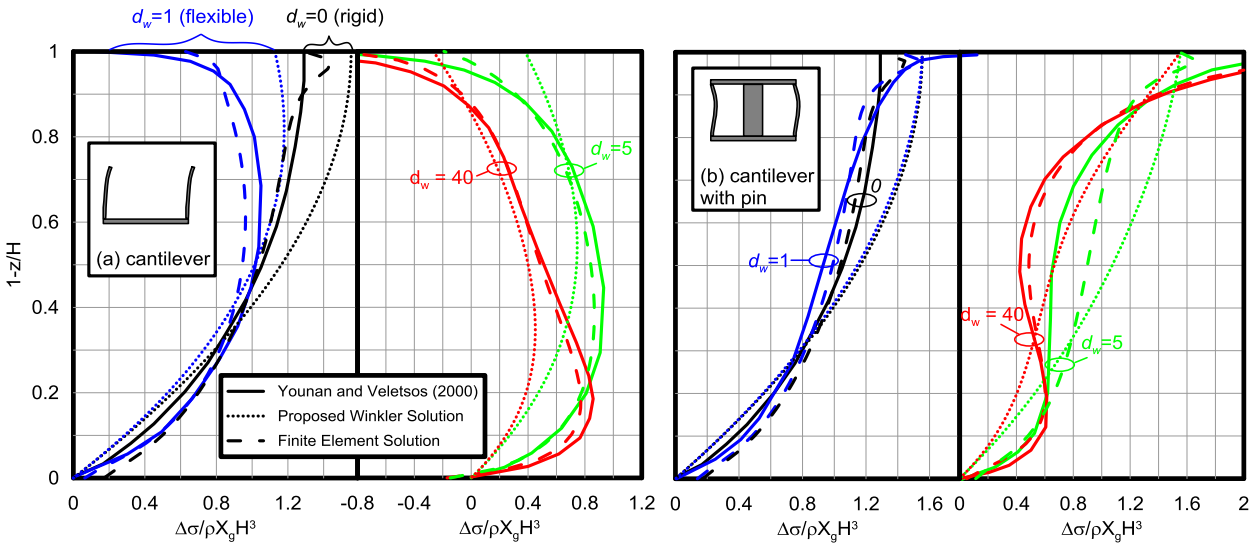

Figure 6. Comparison of proposed Winkler solution with Younan and Veletsos (2000) approximate analytical solution, and a finite element solution for a cantilever wall (ν=0.33). (a) cantilever wall, (b) cantilever wall restrained by pin.

Figure 6(b) shows the configuration with a pin connection constraining the top of the wall. Note that the pinned configuration arises only when a top diaphragm connects the top of the wall to intermediate walls or columns that transfer loads to the floor diaphragm. For a case where the top diaphragm serves as a strut spanning the excavation, but is not connected to intermediate structural elements, antisymmetry dictates that a pin should not be present (a condition not mentioned by Younan and Veletsos). The proposed Winkler solution is again higher than the Younan and Veletsos solution for stiff walls. The Younan and Veletsos solution predicts a sharp increase in pressure near the top of the wall, which can be interpreted as an elasticity-driven singularity. This pattern is visible in the finite element solution, but much less pronounced. For flexible walls (d_w=5 and 40), the Younan and Veletsos solution and the finite element solution indicate more oscillation of pressure with depth compared with the proposed Winkler solution, but the overall trends are similar. The key benefit to the proposed Winkler solution compared to the Younan and Veletsos approach is that it is extensible to boundary conditions that are more complicated than the "bathtub" configuration in which the wall and soil rest atop a rigid base layer (e.g., Brandenberg et al. 2015). The purpose of comparing with the Younan and Veletsos solution is to demonstrate the accuracy of the proposed solution so that it may be confidently extended to problems with more complex boundary conditions.

CONCLUSION

Seismic earth pressures mobilized against vertical walls of underground structures are fundamentally related to relative wall-soil displacements, which in turn depend significantly on the flexural stiffness of the wall, soil stiffness, and the translational and rotational constraints

imposed at the top and bottom of the wall. The M-O method and its variants do not account for structural characteristics of the wall, and therefore miss an important aspect of behavior. The problem is fundamentally a soil-structure interaction problem, and should be analyzed as such. Formation of an active wedge is a poor analogy in this case, and procedures that are based on variations of the M-O theory may be erroneous as a result. The authors urge that this long-held paradigm be abandoned for analysis of underground structures, and replaced with SSI procedures that rationally account for the nature of interaction between walls and the surrounding soil.

The proposed Winkler solution is an approximation that compares reasonably well with the more rigorous approximate analytical solution by Younan and Veletsos (2000) and with finite element simulation results. A benefit of the proposed Winkler solution is that it is amenable to structures with flexible base conditions, whereas analytical solutions are generally restricted to rigid base conditions. Furthermore, the proposed Winkler solution is simpler to implement than finite element solutions.

A few limitations of the proposed Winkler solution are acknowledged here. First, shear stiffness of soil tends to increase with depth due to the influence of confining pressure and age. Solutions that consider inhomogeneous soil profiles with shear modulus increasing with depth show that the seismic earth pressure mobilized at the top of the wall tend to be lower than for uniform soil profiles (e.g., Vrettos et al. 2016, Brandenberg et al. 2017). Vertically homogeneous soil profiles were utilized herein because a closed-form solution to the governing ODE can be obtained, whereas closed-form solutions are highly complex when k_y^i is a function of depth (Franklin & Scott 1979, Fradelos 2016). Second, nonlinearity in soil-structure interaction is not considered in the formulations presented herein, but could conceivably be incorporated by either using an equivalent-linear approximation, or by formulating solutions involving pertinent nonlinear k_y^i elements (p-y analysis). Third, the vertical walls studied herein are assumed to behave as elastic flexural beams. Shear deformation may become a significant contributor to the displacement of walls with a small height-to-thickness ratio (e.g., Massone et al. 2006), thereby rendering the flexural beam assumption inappropriate. Finally, walls may yield in flexure before mobilizing the bending moments predicted herein. Whether the predicted flexural demands exceed the section capacity should be checked, and walls that are predicted to yield should be analyzed using a framework that considers elasto-plastic beam behavior.

REFERENCES

Al Atik, L. and Sitar, N. (2010). "Seismic earth pressures on cantilever retaining structures," J. Geotech. & Geoenv. Eng., ASCE, 136 (10), 1324-1333.

Arias, A., Sanchez-Sesma, F.J., and Ovando-Shelley, E. 1981. A simplified elastic model for seismic analysis of earth-retaining structures with limited displacements. In Proceedings

of the International Conference on Recent Advances in Geotechnical Earthquake Engineering and Soil Dynamics, St. Louis, Mo., Vol. 1, pp. 235–240.

Brandenberg, S.J., Mylonakis, G., and Stewart, J.P. (2015). "Kinematic framework for evaluating seismic earth pressures on retaining walls." *J. Geotech. Geoenviron. Eng.*, 141(7).

Brandenberg, S.J., Agapaki, E., Mylonakis, G., and Stewart, J.P. (2017). "Seismic earth pressures exerted on rigid walls by vertically heterogeneous soil using Winkler method." 16th *World Conference on Earthquake Engineering*, Santiago, Chile. Paper No. 1755. Accepted for publication.

Flores-Berrones R, Whitman RV (1982) "Seismic response of end bearing piles" Journal of the Geotechnical Engineering Division, 108(4): 554-569

Fradelos, J.I. (2016). "Stiffness matrices for laterally loaded piles in homogeneous and inhomogeneous soil." Diploma Thesis, University of Patras, Greece (in Greek).

Franklin, J.N., and Scott, R.F. (1979). "Beam equation with variable foundation coefficient." *J. Engrg. Mech.*, ASCE, 105(5), 811-827.

Geraili, M.R., Candia, G., and Sitar, N. (2016). "Seismic earth pressures on retaining structures and basement walls in cohesionless soils." *J. Geotech. Geoenviron. Eng.* 142(10).

Kloukinas, P., Langoussis, M., and Mylonakis, G. (2012). "Simple wave solution for seismic earth pressures on non-yielding walls." *J. Geotech. Geoenviron. Eng.*, 138(12), 1514-1519.

Massone, L.M., Orakcal, K. and Wallace, J.W. (2006), "Modeling flexural/shear interaction in RC walls", ACI-SP-236, Deformation capacity and shear strength of reinforced concrete members under cyclic loadings, American Concrete Institute, Farmington Hills, MI Paper 7, 127-150.

Mononobe, N. and Matsuo, M. (1929). "On the determination of earth pressures during earthquakes." Proc. World Engrg. Congress, 9, 179–187.

Okabe, S. (1924). "General theory of earth pressure and seismic stability of retaining wall and dam." J. Japanese Society of Civil Engineering, 12 (4), 34-41.Ostadan, F. (2005). "Seismic soil pressure for building walls – an updated approach," Soil Dyn. Earthquake Eng., 25, 785-793.

Papazafeiropoulos, G. and Psarropoulos, P. N. (2010). "Analytical evaluation of the dynamic distress of rigid fixed-base retaining systems", Soil Dynamics & Earthquake Engineering, 30, 12, 1417-1550

Rovithis, E.N., Parashakis, H., and Mylonakis, G.E. (2011). "1D harmonic response of layered inhomogeneous soil: Analytical investigation." *Soil Dyn. And Earthquake Eng.* 31, 879-890.

Seed, H.B. and Whitman, R.V. (1970). "Design of earth retaining structures for dynamic loads." Proc., ASCE Specialty Conf. on Lateral Stresses in the Ground and Design of Earth Retaining Structures, Vol. 1, pp. 103-147, Cornell Univ., Ithaca, NY.

Veletsos A.S. and Younan, A.H. (1994). "Dynamic soil pressures on rigid retaining walls." Earthquake Eng. Struct. Dyn., 23 (3), 275-301.

Vrettos, C., Beskos, D.E., and Triantafyllidis, T. (2016). "Seismic pressures on rigid cantilever walls retaining elastic continuously non-homogeneous soil: An exact solution." *Soil Dyn. And Earthquake Eng.* 82, 142-153

Wood, J.H. (1973). "Earthquake induced soil pressures on structures," Report No. EERL 73-05, California Institute of Technology, Pasadena, CA.

Younan, A.H., and Veletsos, A.S. (2000). "Dynamic response of flexible retaining walls." *Earthquake Eng. And Struct. Dyn*. 29, 1815-1844.